Available online at www.sciencedirect.com
ScienceDirect
Ceramics International 34 (2008) 563–571
CERAMICS INTERNATIONAL
www.elsevier.com/locate/ceramint

The influence of the synthesis route on the final properties of SnO_2-based varistors

R. Parra [a,*], J.E. Rodríguez-Páez [b], J.A. Varela [c], M.S. Castro [a]

[a] *Instituto de Investigaciones en Ciencia y Tecnología de Materiales (INTEMA, CONICET-UNMdP), J.B. Justo 4302, B7608FDQ Mar del Plata, Argentina*
[b] *Grupo de Ciencia y Tecnología de Materiales Cerámicos (CYTEMAC, UNICAUCA), Calle 5 N° 4-70 Popayán, Colombia*
[c] *Instituto de Química, UNESP, PO Box 355, 14801-970 Araraquara, SP, Brazil*

Received 3 July 2006; received in revised form 28 October 2006; accepted 17 December 2006
Available online 30 January 2007

Abstract

A comparative study of two customary routes of ceramics processing applied to the synthesis of SnO_2-based varistors is reported in this paper. Devices of equivalent composition were prepared through the Pechini method and through directly mixing the oxides without the addition of anti-agglomerants or binders. The microstructures of the sintered samples were characterised with X-ray diffraction and scanning and transmission electron microscopies. The electrical behaviour of the devices was studied on the basis of the current density versus electric field (*J–E*) characteristics and impedance spectroscopy measurements. The Pechini method ensures the homogeneity in the distribution of the additives in the tin oxide matrix but the formation of secondary phases seems to be independent of the synthesis route. Devices with similar non-linear coefficients of 18 and 21 were obtained through the mixed oxides route and the Pechini method, respectively.

Keywords: A. Powders: chemical preparation; D. Tin oxide; E. Varistors; Pechini

1. Introduction

Metal oxide varistors are electronic ceramic devices whose function is to sense and limit transient voltage surges and to do so repeatedly without being destroyed or damaged [1,2]. Their non-linear current–voltage behaviour is described by the equation $I = V^{\alpha}$, where α is the non-linearity coefficient whose magnitude is strongly influenced by the addition of transition metal oxides to the varistor composition [3,4]. Surge arresters based on tin dioxide have been reported for the first time in 1995 by Pianaro et al. and, since then, a great deal of research has been done. SnO_2 is an n-type wide band gap semiconductor with a very low densification rate due to its high surface diffusion at low temperatures and high SnO_2 partial vapour pressure at sintering temperatures [5]. Significant improvements in the sinterability of this oxide have been reached by doping with Co_2O_3 and MnO_2 among other oxides [6,7].

Currently, SnO_2-varistors are produced by different processes usually followed to obtain ceramic materials. However, the final properties of the devices are strongly influenced by the selected method. It is said that the standard method of mixing the oxides followed by ball milling is not adequate for advanced ceramic applications. Problems of poor sintering due to large powder agglomerates and non-homogeneities such as minority phases or abnormal grain growth may arise. Besides, the difficulties encountered in achieving a homogeneous mixture of oxides are associated to the imprecise control of stoichiometry and cation distribution. Consequently, the electrical and mechanical properties of the sintered product can suffer and may not match to those expected [8].

On the other hand, the use of polymeric precursors in the synthesis of ceramic materials is believed to have significant advantages. The synthesis route developed by Pechini in 1967 consists in a clever method that ensures the homogeneity in the distribution of the additives in the final piece. The process involves the use of polymeric precursors and is based on the ability of certain α-hydroxycarboxylic acids to form chelates with metallic cations. When heated in the presence of a

* Corresponding author.
E-mail address: rparra@fi.mdp.edu.ar (R. Parra).

0272-8842/$34.00
doi:10.1016/j.ceramint.2006.12.003

polyhydroxy alcohol, these chelates undergo polyesterification with the cations randomly distributed throughout the resulting polymer structure. The ignition of the resin removes the organic material and leaves the desired composition of mixed oxides, chemically combined and in a finely divided state, as the residue [9]. The organic precursors also provide the combustion heat for calcinations; therefore, if an excess of organics is used, the temperature during calcinations may be raised above the set point. The high temperature would lead to large crystallites and hard agglomerates of particles [8].

The purpose of this work is to consider two of the most frequent routes of ceramics processing applied to the synthesis of SnO_2-based varistors to clarify their influence on the microstructure development and to evaluate the electrical behaviour and the goodness of devices obtained through different methods. A discussion is addressed after the characterisation of the starting powders and of the microstructure and electrical response of sintered pellets.

2. Experimental procedure

2.1. Sample preparation through the mixing of oxides route

Analytical grades of SnO_2 (Aldrich), Co_3O_4 (Merck), Nb_2O_5 (Fluka AG), Fe_2O_3 (Baker) and La_2O_3 (Anedra) were used as precursors for processing SnO_2-based varistors according to the compositions listed in Table 1. After mixing the powders in an alcoholic medium (2-propanol) by stirring with a high-speed turbine at 6000 rpm for 5 min, the slurries were kept at 65 °C for 48 h until constant weight. The mixtures were sieved through a 43 μm mesh screen and then uniaxially pressed at 150 kg/cm^2 into pellets of a diameter around 12 mm and 1 mm in thickness. Finally, the pellets were sintered in air at 1300 °C for 2 h with heating and cooling rates of 3 °C/min in a Carbolite RHF17 furnace.

2.2. Sample preparation through the Pechini method

Analytical grades of $SnCl_2{\cdot}2H_2O$ (Baker), $Co(OCOCH_3)_2{\cdot}4H_2O$ (Acros Organics), $La(OCOCH_3)_3{\cdot}xH_2O$ (Aldrich) and $Fe(NO_3)_3{\cdot}9H_2O$ (Sigma) were employed as sources of the cations of interest. Due to the unavailability of water-soluble salts of niobium at a reasonable cost, niobium was added as a fine dispersion of its oxide (Nb_2O_5; Fluka AG 99.9%). The selected compositions are listed in Table 1. Tin dioxide was precipitated at pH 6.25 through the drop-wise addition of ammonium hydroxide (NH_4OH) to an acidic (HNO_3) solution of tin(II) chloride. It is known that the chloride species present in the medium have detrimental effects on the microstructure of the final material; a series of washings with a deionised water solution of diethylamine were carried out until negative reaction of the filtrate with a concentrated silver nitrate ($AgNO_3$) solution. The obtained slurry, along with the required amounts of the dissolved additives, was added to a solution of citric acid in ethylene glycol in a 1:4 molar ratio. The mixtures were left at room temperature with constant stirring for a 24 h aging with the purpose of promoting the formation of the metallic citrates. Later, a concentrated solution of NH_4OH was slowly added until a transparent solution was attained which was afterwards evaporated and heated in order to produce an amorphous organic polymer. This solid was heated to 350 °C for 12 h in the beaker to burn off as much of the organics as possible. The resulting black brittle mass was ground, transferred into an alumina crucible of large surface and calcined in an oven at 650 °C for 4 h. The remaining powder, which consisted in the mixture of oxides with the desired composition, were dispersed in pure ethanol and attrition milled with ZrO_2 balls to disintegrate large particles and agglomerates and to maximise the homogeneous distribution of Nb_2O_5 in the calcined powder. Pellets of approximately 12 mm and 1 mm in diameter and thickness, respectively, were obtained by uniaxial pressing of the powders at 150 kg/cm^2. Finally, the pellets were sintered in air at 1300 and 1350 °C for 2 h with heating and cooling rates of 3 °C/min in a Carbolite RHF17 furnace.

Table 1
Sample composition

	SnO_2	Co_3O_4	Nb_2O_5	Fe_2O_3	La_2O_3
SCN	99.62	0.33	0.05	–	–
SCNF	99.52	0.33	0.05	0.10	–
SCNL	99.52	0.33	0.05	–	0.10

Values in mol%.

2.3. Characterisation techniques

The specific surface area (BET-ASAP) of the powders was determined with a Micromeritics ASAP 2010 instrument. The apparent density of sintered samples was estimated by the Archimedes method. X-ray powder diffraction (XRD) analysis was carried out with a Philips PW 1830/40 equipment running with Co Kα radiation.

The powders prepared through the Pechini method were studied with transmission electron microscopy (TEM) in a Jeol JEM 1200EX microscope and by scanning electron microscopy in a Zeiss-Supra35 equipped with a field emission gun (SEM-FEG). The microstructural characterisation of the sintered samples was performed by SEM, in a Topcon SM300 microscope, and by TEM, in a Philips CM200 instrument operating at 200 kV. These SEM and TEM instruments were equipped with an EDS (PGT) system for energy dispersive X-ray analysis. Average grain sizes were estimated from SEM micrographs through the method of the interceptions [10].

The sintered samples were lapped to ensure plane parallel faces where silver electrodes were painted for electrical characterisation. A Keithley 237 high voltage source-measure unit was used to acquire plots of the current density (J) as function of the electric field (E) at room temperature. The electrical breakdown field was measured at 1 mA/cm^2 and, assuming that the grain boundary breakdown value is compatible with the SnO_2 band gap of 3.5 V, the percentage

of electrically active barriers (EAB) in each sample was determined as

$$\%\text{EAB} = \frac{V_b}{3.5} \times 100, \quad (1)$$

with

$$V_b = V_r \frac{d}{e}, \quad (2)$$

where V_b is the breakdown voltage per barrier, V_r the breakdown voltage of the device measured at 1 mA/cm^2, e the sample thickness and d is the average grain size.

Impedance spectroscopy (IS) measurements were carried out by means of an HP4284A LRC meter with an amplitude voltage of 0.5 V in the frequency range of 20 Hz to 1 MHz. Curves of the imaginary ($-Z''$) versus the real (Z') component of impedance were acquired at 120 °C in order to obtain the grain boundary resistance (R_{gb}) and capacitance (C_{gb}).

3. Discussion

3.1. Samples prepared through mixing the oxides

3.1.1. Microstructural properties

The sintered samples obtained through the mixing of oxides route, –MO samples, did not show the presence of secondary phases under XRD resolution. A specific surface area of 7.2 m^2/g and a mean particle size below 300 nm were measured for the precursor powders. A representative SEM image of the SCNF–MO powder is shown in Fig. 1. Only SnO_2 was detected during the EDS analysis of the powders suggesting the homogeneous distribution of the additives. Although a broad particle size distribution is inferred from this picture, it is not different from what can be seen in the undoped-SnO_2 powder dispersed in 2-propanol and dried at 65 °C.

Fig. 2 shows the homogeneous microstructures, apparently without the presence of secondary phases, achieved after a thermal treatment at 1300 °C for 2 h. It can be seen in Table 2 that the average grain size of the sample SCN–MO increased with the addition of iron oxide (Fe_2O_3) to the SCN composition. Although in a minor extent, the grain size also increased in the presence of La_2O_3; however, the density diminished with respect to that of the SCN–MO sample. According to previous results [11], the replacement of Sn^{4+} by Fe^{2+} or Fe^{3+} during the solid solution formation increases the concentration of oxygen

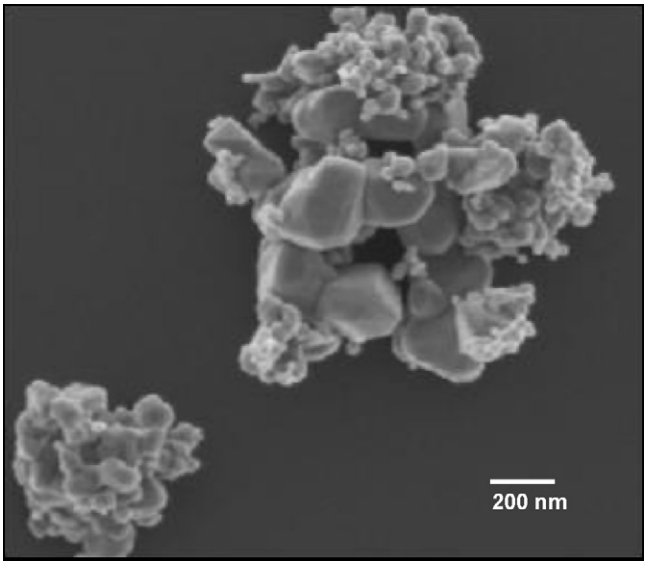

Fig. 1. SEM–FEG image of the precursor powder for the SCNF–MO sample.

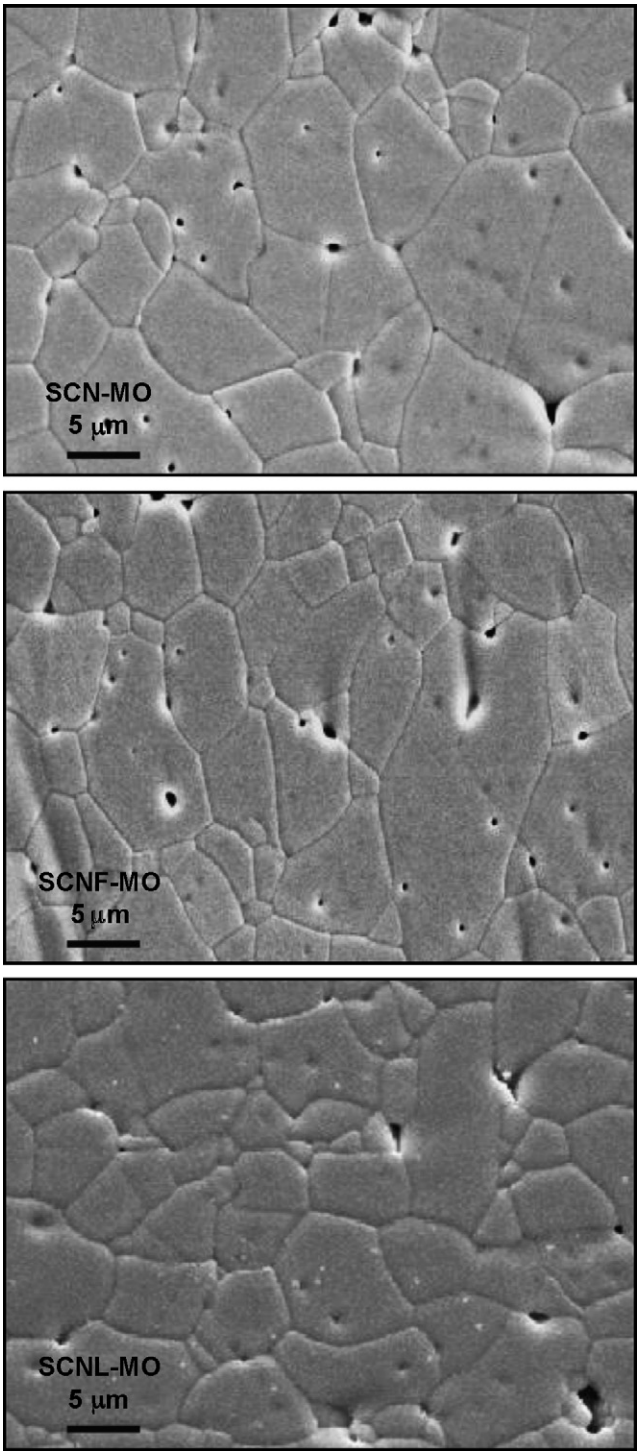

Fig. 2. SEM images of the sintered samples obtained through the mixing of oxides route.

Table 2
Percentage of SnO_2 theoretical density (ρ_t), mean grain size (d), electric breakdown field (E_b), non-linearity coefficient (α), grain boundary resistance (R_{gb}) and percentage of electrically active barriers of sintered samples (EAB)

	ρ_t (%)	d (μm)	E_b (V/cm)	α	R_{gb} (Ω)	EAB (%)
SCN–MO	98.0	5.0	2090	14	1.8×10^5	30
SCNF–MO	98.0	5.8	3440	18	4.0×10^6	57
SCNL–MO	97.4	5.3	2900	17	1.6×10^6	44
SCN–P	95.0	5.5	3908	15	$>3 \times 10^7$	58
SCNF–P	96.4	6.9	4630	21	$>7 \times 10^7$	90
SCNL–P	94.5	5.5	3745	18	N/A	53

–MO: mixture of oxides; –P: Pechini; SnO_2 theoretical density: 6.95 g/cm^3.

vacancies, species that stimulate the solid-state diffusion at sintering temperatures. On the other hand, the solubilization of La_2O_3 in SnO_2 is limited by the difference between the ionic radii of Sn^{4+} (0.71 Å) and La^{3+} (1.15 Å).

Interestingly, the analysis with TEM revealed the presence of particles of secondary phases in every –MO sample. The EDS spectrum of the particles detected in the sample SCNF–MO (Fig. 3a) shows that they are composed of Sn, Co, Fe and O. The presence of a cobalt and iron stannate of the formula $Co_{1.5}FeSn_{0.5}O_4$ has been reported in varistor systems with 0.05 mol% of Fe_2O_3 [12]. The small particles found in sample SCNL–MO did not include lanthanum in their composition but Sn, Co and O only (Fig. 3b). In this work, and as also exposed in the related literature [13], lanthanum has proven a low reactivity towards the formation of compounds with SnO_2 with respect to Co and Fe. Therefore, lanthanum oxide preferentially segregates at grain boundaries from where it hinders the grain growth.

3.1.2. Electrical behaviour

Fig. 4a and b shows the *J–E* characteristics of the –MO samples at room temperature and the impedance curves obtained at 120 °C, respectively, whereas the Table 2 lists the usual parameters derived from these curves. The effect of the addition of Fe_2O_3 and La_2O_3 on the SCN–MO system was to increase the breakdown voltage, the non-linearity coefficient, the grain boundary resistance and the percentage of electrically active barriers. The enhancement of the electrical behaviour of sample SCN–MO can be attributed to the segregation of point defects and ions to grain boundaries where they induce changes in the concentration of the atomic defects at grain–grain junctions [14]. If Schottky type electrical barriers are supposed to form at grain boundaries, the negative surface charge at the interface separating two grains is compensated with positive charges in the depletion layers on both sides of the interface. This atomic defects model involves positively charged donors ($V_O^{\bullet\bullet}$, $V_O^{\bullet}$, $Nb_{Sn}^{\bullet}$) located at the depletion layers and negatively charged acceptors (Fe''_{Sn}, Fe'_{Sn}, La'_{Sn}, Co'_{Sn}, Co''_{Sn}, V''_{Sn}, V''''_{Sn}, O', O'') at the grain boundaries interface [14].

The occurrence of secondary phases that concentrate the additives is a further factor that modifies the expected electrical properties. The creation of adjacent regions at grain boundaries with uneven concentrations of segregated metal atoms in

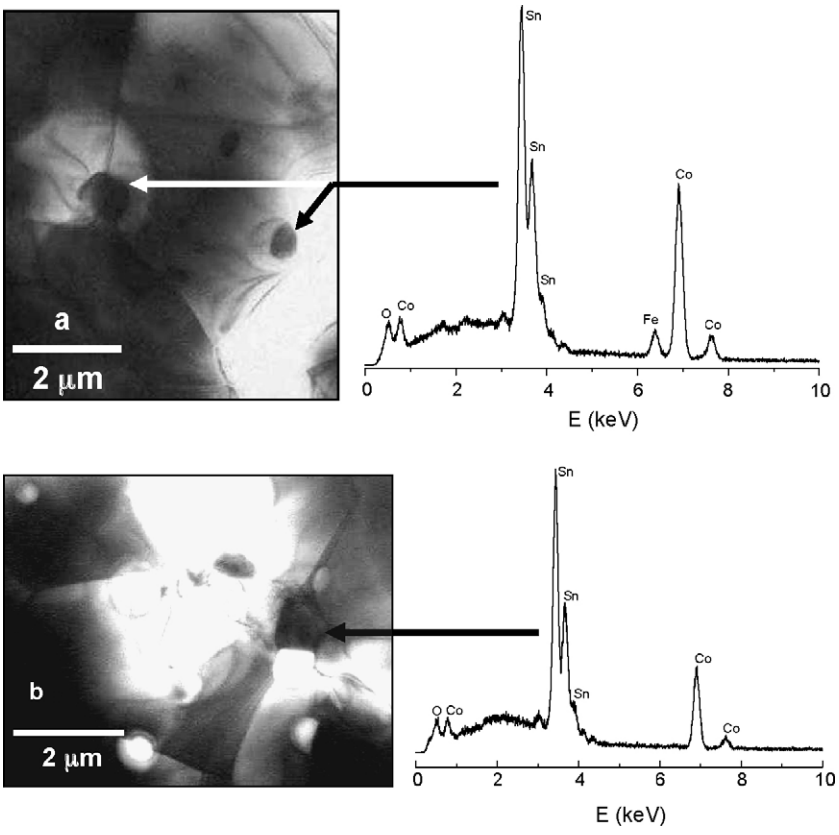

Fig. 3. TEM image of samples: (a) SCNF–MO and (b) SCNL–MO showing particles of secondary phases (arrowed) and the EDS spectra of those particles.

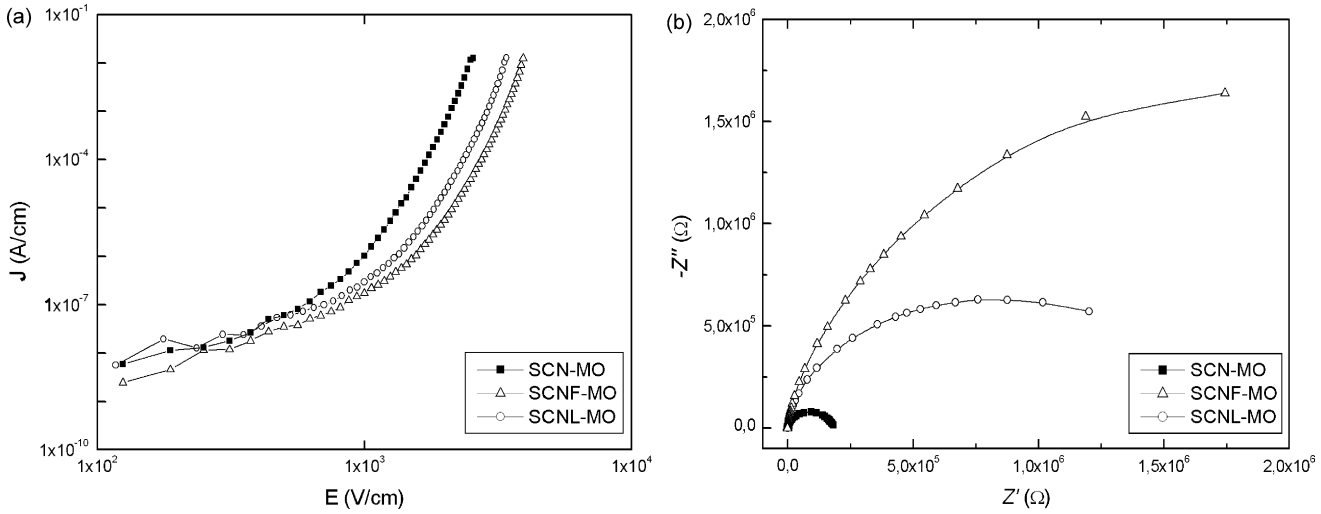

Fig. 4. (a) *J–E* characteristics and (b) impedance spectroscopy curves of the sintered samples obtained by means of mixing the oxides.

systems with an excessive amount of precipitates has been suggested to be deleterious to the non-ohmic properties of SnO_2 varistors [15]. In fact, precipitates of secondary phases concentrate the species intentionally added to enhance the varistor properties and the control of the incorporation of dopant ions into the host lattice is lost. They also reduce the number of electrically active barriers originating preferential paths for the electron flow and, therefore, they diminish the quality of the device.

3.2. Samples prepared through the Pechini method

3.2.1. Microstructural properties

Fig. 5 corresponds to the TG plot of the black mass pre-calcined at 350 °C during 12 h. According to this curve, the calcination temperature was fixed in 650 °C. The XRD pattern of the resulting powder is shown in Fig. 6 in which the signals of SnO_2 – cassiterite (JCPDS 41-1445) – are recognised. The morphology of the particles that build up the powders, before and after being attrition milled, is presented in Fig. 7a and b, respectively. Initially, the presence of large crystals or grains determined a broad particle size distribution with a specific surface area of 9 m^2/g; but, after being milled, a relatively homogeneous distribution was achieved and the ASAP assay yielded a surface area of 25 m^2/g. As can be seen in Fig. 7c, the small size of the particles is responsible for their agglomeration. However, as seen with TEM (Fig. 7d), the particles are loosely bonded. The formation of agglomerates may be controlled by the addition of charged species such as amino acids in the initial steps of synthesis. The presence of chlorine ions from the $SnCl_2$ precursor might also contribute to the non-occurrence of agglomerates by constituting a negatively charged film around SnO_2 nanocrystals that prevents particles from growing or agglomerating. However, chlorine ions would also impede the densification during sintering. Another possibility to avoid powder agglomeration implies the lowering of the calcination temperature. However, a situation of compromise arises; the

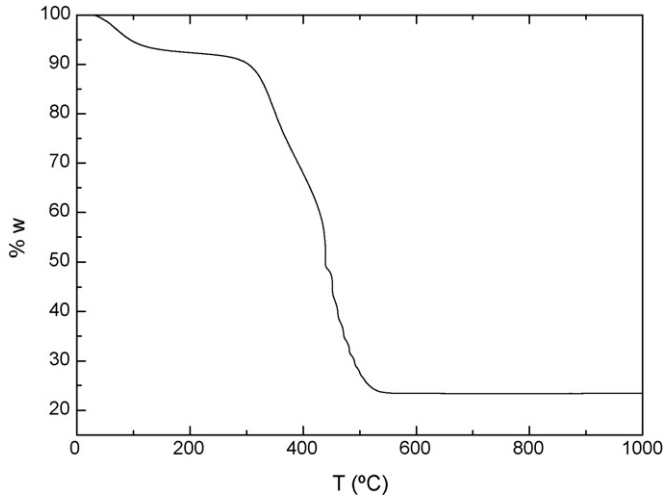

Fig. 5. TG curve of the powder of composition SCN obtained through the Pechini method.

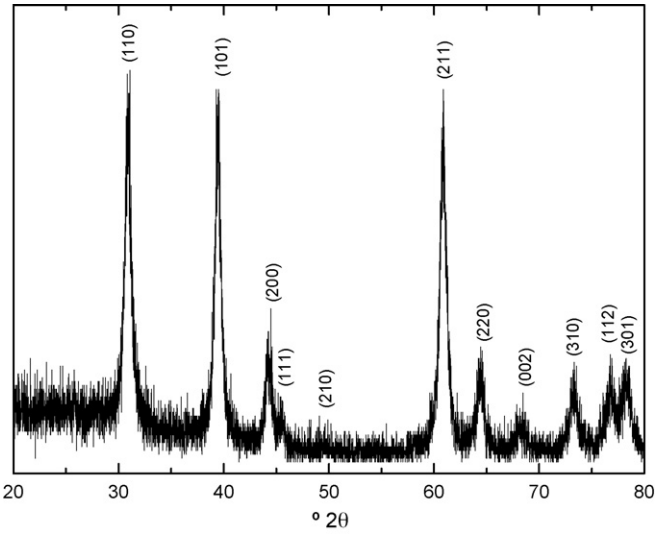

Fig. 6. XRD pattern of the powder of composition SCN obtained through the Pechini method treated at 650 °C for 4 h.

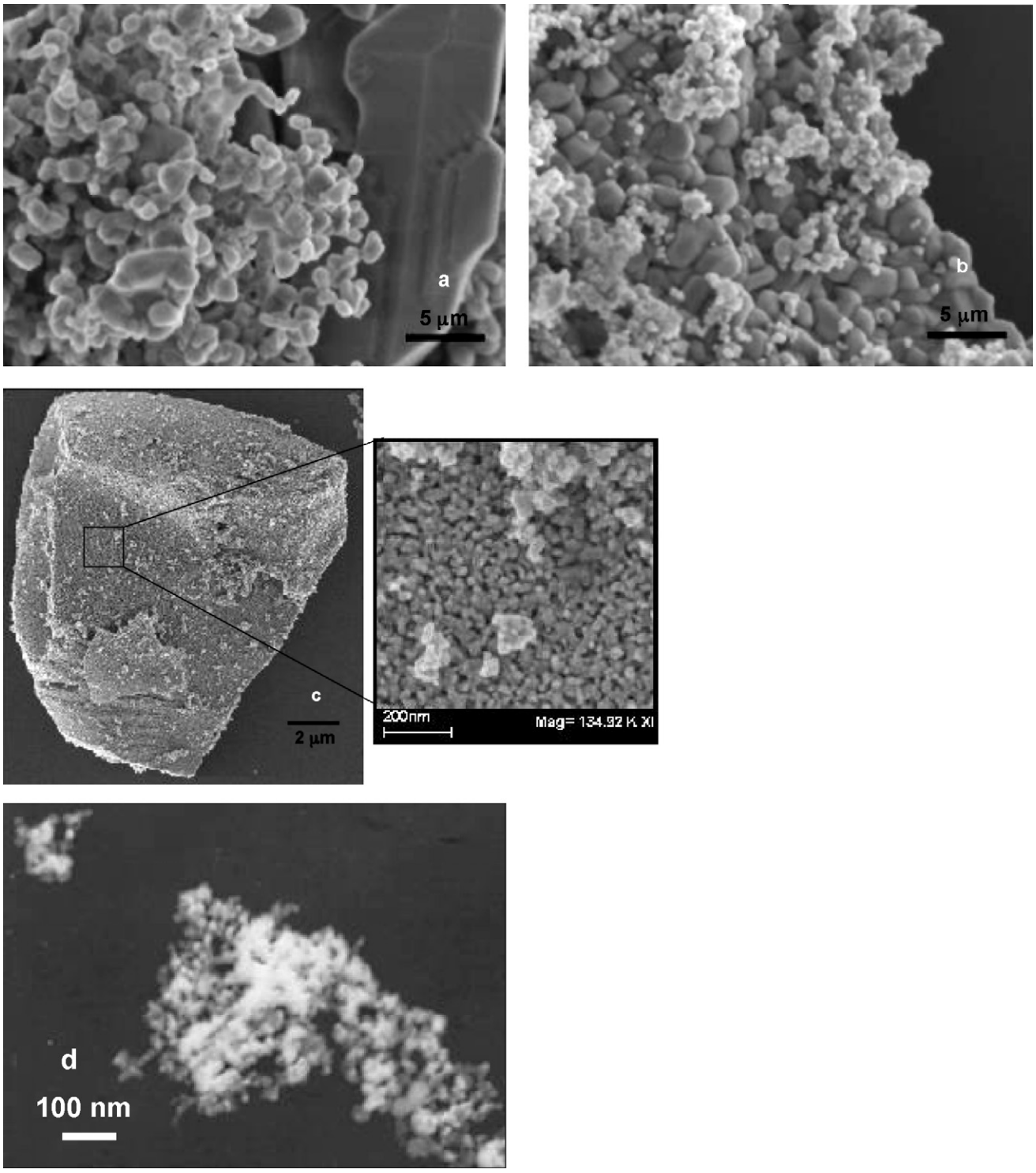

Fig. 7. SEM–FEG images of the powders obtained through the Pechini method: (a) before and (b) after milling, (c) image of a dense agglomerate of nano-particles in the milled powder and (d) TEM image of loosely bonded particles in the milled powder.

residual carbon content in the calcined powder is undesirable and low calcinations temperatures may not be sufficient to burn all the organics.

Samples sintered at 1300 °C led to densities below the 85% of the theoretical density of SnO_2 maybe due to the presence of large agglomerates of fine particles. The shrinkage of agglomerates may lead to large pores which are more difficult to eliminate. Then, in order to achieve density values alike those measured for the –MO samples, it was necessary to increase the sintering temperature in 50 °C. The SEM images of the polished samples sintered at 1350 °C are shown in Fig. 8, and Table 2 lists the average grain sizes and the percentage of the theoretical density of SnO_2. It can be seen that Fe and La modified the microstructure in different ways. Due to their ionic

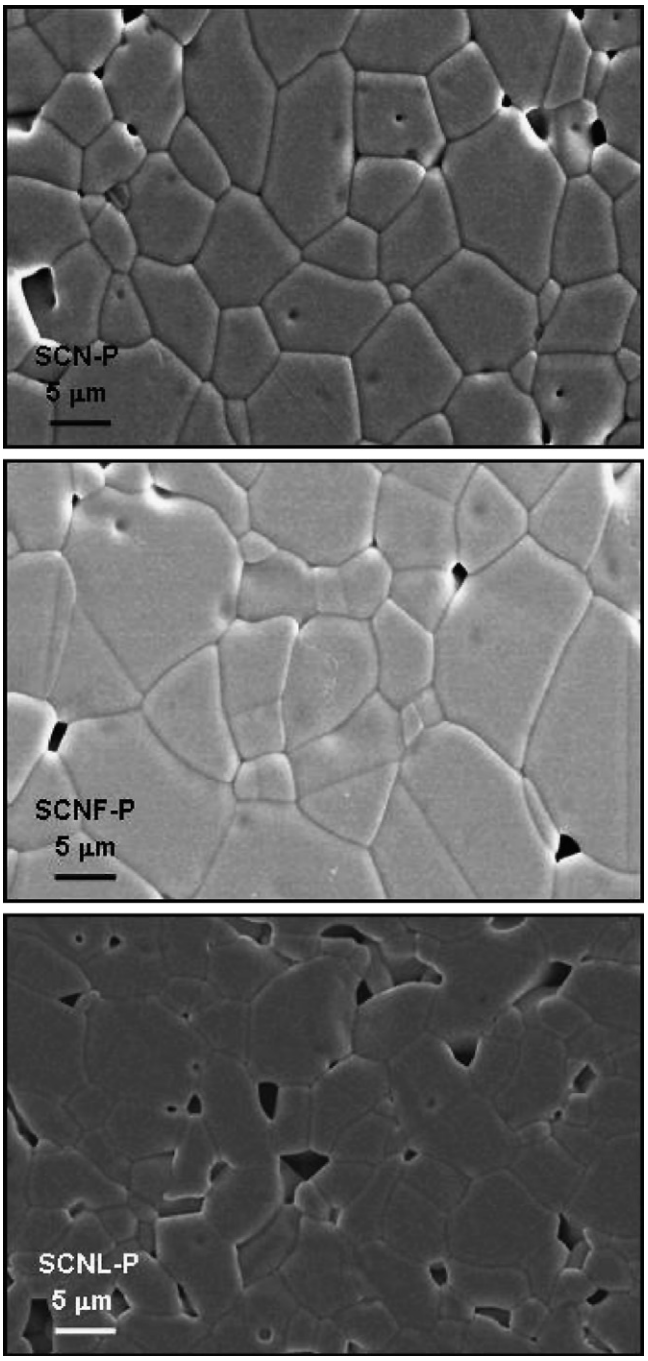

Fig. 8. SEM images of the sintered samples obtained through the Pechini method.

radii, Fe^{3+} and Fe^{2+} species are able to form a solid solution with SnO_2 accompanied by the creation of oxygen vacancies that enhance the densification and grain growth. On the other hand, La^{3+} ions segregate on the surface of the grains and hinder the growing of the tin oxide grains. In fact, the higher porosity of the sample SCNL–P is evident in Fig. 8.

The Pechini samples, –P samples onwards, showed lower densities than the –MO systems which, in contrast, were sintered at a lower temperature. The presence of large agglomerates and consolidated particles in the calcined powder is believed to be the main reason for this observation. Another possibility that hinders the material densification may be the presence of traces of chlorine ions in the surface of SnO_2 particles. On the other hand, the average grain sizes are larger for –P samples due to the higher sintering temperature with respect to that employed for –MO samples and, also due to the smaller average size of the particles that compose the milled powder what, as well as the temperature, constitutes the driving force for grain growth. Besides, the Pechini method provides a medium that maximises the contact between the additives and facilitates the substitution reactions of Sn^{4+} by the dopant species, and consequently, the creation of oxygen vacancies that stimulate the grain growth. However, the presence of agglomerates may lead to a poor densification during sintering.

The X-ray diffraction patterns of the sintered –P samples did not reveal the presence of secondary phases besides SnO_2, as well as in the samples prepared through mixing the oxides. However, particles of minority phases were detected with TEM as seen in Figs. 9 and 10 for samples with Fe and La, respectively, together with the elemental analysis of both the matrix and the observed particles. It can be seen that at least two different minor phases are present. In the sample with iron, particles composed of Sn, Co, Fe and O have been found, whereas the particles detected in the sample with lanthanum are only composed of Sn, Co and O. It is clear that the formation of such minority phases is unavoidable and it obeys to the chemical nature of the additives and to the excess energy provided during the sintering stage. The absence of lanthanum in these secondary phases confirms once more the lower affinity of La towards the reaction with SnO_2 to render possible lanthanum stannates. Although niobium was added as an alcoholic dispersion of Nb_2O_5, it was not found to nucleate other minority phases. Then, even if the Pechini method ensures the homogeneity in the distribution of the additives, actually, it does not provide advantages regarding the formation of secondary phases.

3.2.2. Electrical behaviour

As shown in Table 2 and in Fig. 11, the electrical behaviour of the sample SCN–P was improved with the addition of 0.2 mol% of Fe^{3+}. The non-linear coefficient α was increased from 15 to 21 and the percentage of electrically active barriers was increased from 58 to 90%. Considering that the average grain size of the sample SCNF–P is higher than that of the sample SCN–P, the higher E_r and R_{bg} of the former confirm that the addition of iron enhances the intergranular barrier properties. On the other hand, the *J–E* characteristics curves of samples SCN–P and SCNL–P are almost superposed and the improvements are rather negligible. In fact, the exceptionally high porosity of the sample with lanthanum made it impossible to establish an approximate R_{gb} value; a huge dispersion between several samples of the same composition was observed. The presence of particles that put aside the additives may be another factor that impoverishes the electrical properties. Due to the low density and to the presence of secondary phases that do not allow to guarantee the composition, each sample owns its unique characteristics and it is not possible to reproduce the same behaviour between

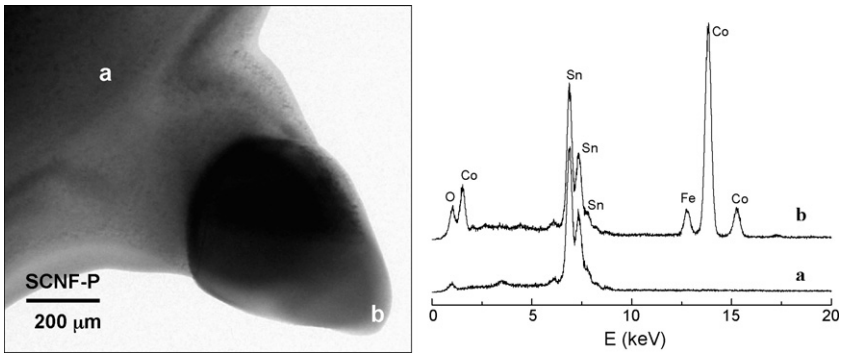

Fig. 9. TEM image of the sintered sample SCNF–P showing a particle of the minority phase and the EDS spectra of (a) the matrix and (b) of secondary phase detected.

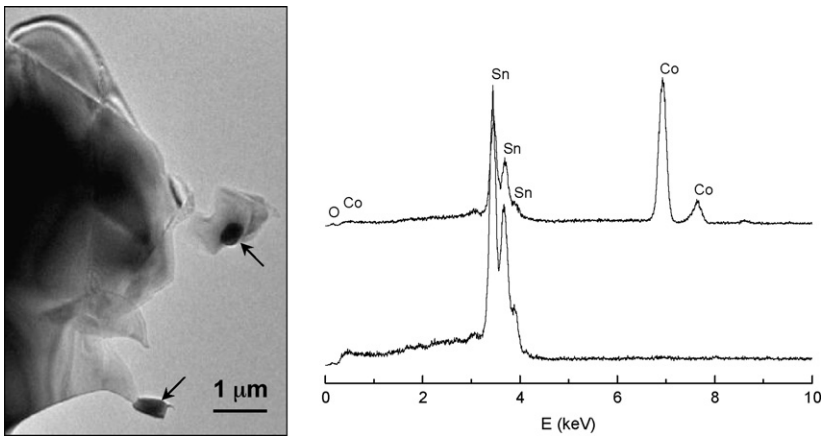

Fig. 10. TEM image of the sintered sample SCNL–P showing particles of minority phases (arrowed) and the EDS spectra of (a) the matrix and (b) of the secondary phase detected.

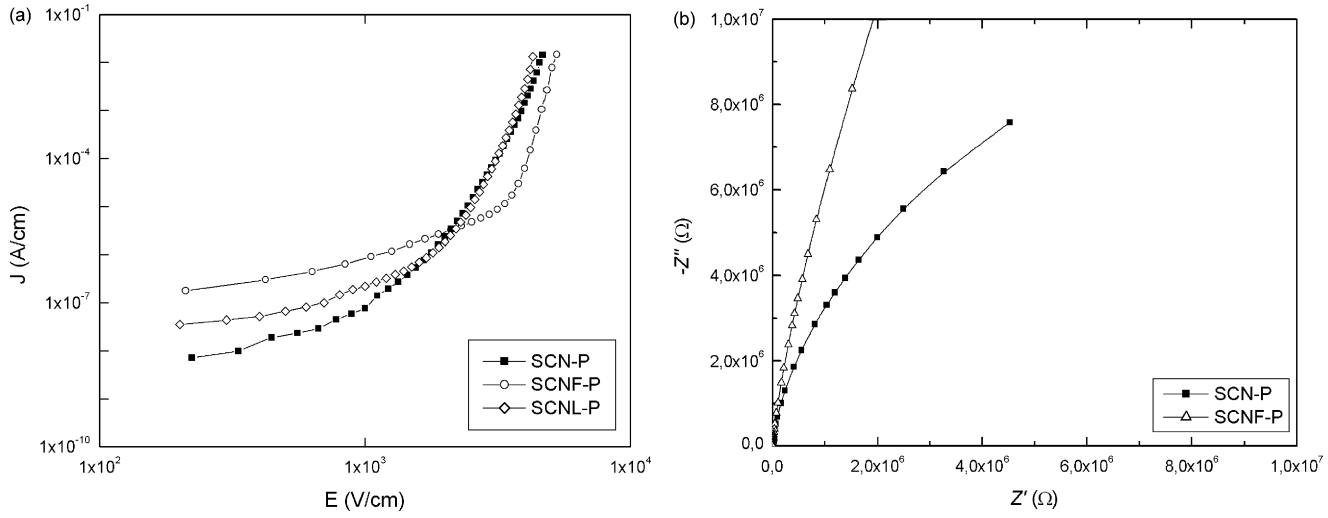

Fig. 11. (a) *J–E* characteristics and (b) impedance spectroscopy curves of the sintered samples obtained through the Pechini method.

samples prepared in the same way. The electrical behaviour is intimately related to the microstructure of the material.

4. Conclusions

The experimental results here reported brought to light the differences that exist between SnO_2-based varistors obtained through two of the most traditional routes employed in the processing of ceramic materials. The differences observed in the developed microstructures are attributable to the different morphology of the precursor powders. However, the arising of particles of secondary phases in the sintered samples seems to be unavoidable independently of the synthesis method. Then, the Pechini method ensures the homogeneity in the distribution

of the additives though it does not provide advantages regarding the formation of undesired phases. This technique enhances the effects of the additives; then, if the behaviour displayed by the samples prepared through the mixing of oxides route is to be reproduced by the Pechini method, the compositions must be optimized.

The Pechini method leads to a more homogeneous distribution of point defects at grain boundaries that allows a higher number of electrically active barriers. On the other hand, the mixing of oxides route led to samples with lower electric breakdown fields; however, the non-linear coefficients are similar to those of the Pechini samples. Although the final density of the devices should be improved, the SCNF–P samples displayed non-linear electrical behaviour and a high percentage of electrically active barriers.

Acknowledgements

The authors are grateful to the Programa CYTED, to CONICET (Argentina), to COLCIENCIAS Cod.1103-14-17900 (Colombia) and to CNPq and FAPESP (Brasil) for the financial support provided for this research. Thanks are also given to P. Mosquera from the Laboratory of Electron Microscopy of the UNICAUCA, Popayán, Colombia, to Y. Maniette for TEM at the IQ, UNESP, Brasil and to M.O. Orlandi for SEM-FEG at the LIEC, UFSCar, Brasil.

References

[1] L.M. Levinson, H.R. Philipp, Zinc-oxide varistors—a review, Am. Ceram. Soc. Bull. 65 (1986) 639–646.
[2] M. Matsuoka, Progress in research and development of zinc oxide varistors, in: L.M. Levinson (Ed.), Grain Boundary Phenomena in Electronic Ceramics, Advances in Ceramics, vol. 1, The American Ceramic Society Inc., Ohio, 1981, pp. 290–308.
[3] T.K. Gupta, Application of zinc oxide varistors, J. Am. Ceram. Soc. 73 (1990) 1817–1840.
[4] S.A. Pianaro, P.R. Bueno, E. Longo, J.A. Varela, Microstructure and electric properties of a SnO_2 based varistor, Ceram. Int. 25 (1999) 1–6.
[5] J.A. Varela, L.A. Perazolli, E. Longo, E.R. Leite, J.A. Cerri, Effect of atmosphere and dopants on sintering SnO_2, Radiat. Eff. Def. Solids 146 (1998) 131–143.
[6] S.A. Pianaro, P.R. Bueno, E. Longo, J.A. Varela, A new SnO_2-based varistor system, J. Mater. Sci. Lett. 14 (1995) 692–694.
[7] M.S. Castro, C.M. Aldao, Characterization of SnO_2-varistors with different additives, J. Eur. Ceram. Soc. 18 (1998) 2233–2239.
[8] P.A. Lessing, Mixed-cation oxide powders via polymeric precursors, Ceram. Bull. 68 (1989) 1002–1007.
[9] M.P. Pechini, Method of preparing lead and alkaline-earth titanates and niobates and coating method using the same to form a capacitor, US Patent No. 3,330,697, July 11, 1967.
[10] M.I. Mendelson, Average grain size in polycrystalline ceramics, J. Am. Ceram. Soc. 52 (1969) 443–446.
[11] R. Parra, M.S. Castro, J.A. Varela, Analysis of secondary phases segregated and precipitated in SnO_2-based varistors, J. Eur. Ceram. Soc. 25 (2005) 401–406.
[12] R. Parra, C.M. Aldao, J.A. Varela, M.S. Castro, The role of oxygen vacancies on the microstructure development and on the electrical properties of SnO_2-based varistors, J. Electroceram. 14 (2005) 149–156.
[13] M.M. Oliveira, P.C. Soares Jr., P.R. Bueno, E.R. Leite, E. Longo, J.A. Varela, Grain-boundary segregation and precipitates in La_2O_3 and Pr_2O_3 doped-SnO_2·CoO-based varistors, J. Eur. Ceram. Soc. 23 (2003) 1875–1880.
[14] P.R. Bueno, E.R. Leite, M.M. Oliveira, M.O. Orlandi, E. Longo, Role of oxygen at the grain boundary of metal oxide varistors: a potential barrier formation mechanism, Appl. Phys. Lett. 79 (2001) 48–50.
[15] L.G.P. Simões, P.R. Bueno, M.O. Orlandi, E.R. Leite, E. Longo, The influence of excess precipitate on the non-ohmic properties of SnO_2-based varistors, J. Electroceram. 10 (2003) 63–68.